

## Tri-functional Bio-friendly Cross-linker for UV-Curable Coatings: Synthesis and Study of Viscoelastic Properties

A. Madhi\*, B. Shirkavand Hadavand\*\*

Department of Resin and Additives, Institute for Color Science and Technology, P.O. Box: 1668814811, Tehran, Iran.

### ARTICLE INFO

Article history:

Received: 12 Jun 2020

Final Revised: 12 Sept 2020

Accepted: 15 Sept 2020

Available online: 01 Dec 2020

Keywords:

UV-curable urethane acrylate

Cross-linker

Bio-friendly

Viscoelastic properties

Cross-link density.

### ABSTRACT

*Protection of the environment and keeping it from contaminants are critical issues. Polymers and oil-based plastics are unrenovable and entail a wide range of environmental pollution due to the long degradation. This study aims to synthesize bio-based coatings using natural substances, and evaluate their viscoelastic properties. Accordingly, first, UV-curable tri-functional castor oil-based waterborne urethane acrylate as a bio-friendly cross-linker was synthesized. Next, different weight percentages of the synthesized cross-linker were added to the UV-curable urethane acrylate resin, followed by UV radiation exposure to prepare, different flexible composite coatings. FT-IR spectroscopy was used to examine the progress of the cross-linker synthesis. The particle size analysis confirmed the stability and homogeneous distribution of the cross-linker particles in the emulsion. By DMTA analysis, viscoelastic characteristics of the films were studied. As a result, adding specific weight percentages of cross-linkers to the polymer matrix caused an increase in storage modulus and improvement of  $T_g$  of the coatings. The cross-link density of the film coatings was estimated from DMTA. The more weight percent of the cross-linker, the more is the cross-link density. *Prog. Color Colorants Coat.* 14 (2021), 199-207 © Institute for Color Science and Technology.*

### 1. Introduction

Polymers and composites or eco-friendly nanocomposites are applicable to those kinds of substances which are derived from renewable resources, and degradable in the nature during a short time [1, 2]. Nowadays, concerning the environmental pollution caused by the long degradation of plastic waste, and the high consumption of unrenovable oil resources to produce polymers, scholars and scientists are to find new approaches to get rid of these worries. Designing and synthesizing polymers using renewable natural resources to decrease the usage of oil resources are the best solutions [3, 4].

Polyurethanes as a major group of polymers are utilized in transparent and flexible coatings, hybrid

coatings, adhesives, synthetic leather, and various industries because of their excellent properties such as low toxicity, resistance to erosion, and high mechanical, chemical and thermal resistance [5, 6]. In recent years, the use of curable polymer coatings has interested scholars and industries because of high process velocity, removal of hazardous organic solvents, adapting to the environment, high cure speed in a low temperature, and saving energy [7, 8]. Waterborne polyurethane acrylate resin is a main UV-curable polymer that its oligomer is created by the reaction between isocyanates, di(poly)ols and chain extenders. Diols or polyols used in the synthesis of polyurethanes are prepared from the chemical substances derived from oil and natural gas [9, 10].

\*Corresponding author: \* [abbas.madhi@semnan.ac.ir](mailto:abbas.madhi@semnan.ac.ir)

\*\* [shirkavand@icrc.ac.ir](mailto:shirkavand@icrc.ac.ir)

Because of the difficulties with the plastic waste removing, the importance of using renewable resources is undeniable. The vegetable oils existing in most of the oil seeds are natural, renewable, and low cost resources. In the past few years, the use of natural triglyceride oils as renewable resources in the preparation of resins, composites, and polymer nanocomposites has drawn the scholars and industries attention. These products have economic and environmental benefits compared to the oil-based substances [11, 12].

Triglyceride oils are ester compounds with one glycerol and three fatty acids molecules. In the structure of fatty acids, there could be some groups like epoxy, hydroxyl and double bonds, too. Castor oil is regarded as a vegetable triglyceride and a renewable resource. About 90-95 percent of castor oil consists of an unsaturated fatty acid named ricinoleic acid containing hydroxyl groups, and as a natural polyol could be proper for reaction with isocyanate and carboxyl groups. Therefore, it is a good substance for the synthesis of different polymers including polyurethanes [13-15].

Polymer cross-linkers are significant chemical compounds such as monomers or oligomers with double bonds or functional groups that are the cause of connection and extension of polymer chains through chemical and covalent bonds in three dimensions. Cross-linkers like glycerol and (meth)acrylates include various functional groups including double bonds and hydroxyl groups that extend the polymer networks [16, 17]. The use of cross-linkers in different industries and technologies has attracted a lot of attention. Cross-linkers lead to the improvement of polymer properties including the decrease of viscosity, preserving the shape memory, improvement of mechanical features and viscoelastic behavior, and increase in cross-link density [18-20]. Cross-link density and chemical structure of the polymer chains influence the mechanical and thermal features of the polymers. Increasing the cross-link density is an effective way to improve the mechanical, viscoelastic, and thermal properties of the polymers, composites and nanocomposites [21, 22].

In the current research, first, UV-curable tri-functional castor oil-based waterborne urethane acrylate as a bio-friendly cross-linker was produced. Different weight percentages of the synthesized cross-linker were added to the UV-curable urethane acrylate

resin. The resultant mixtures were exposed to ultraviolet radiation to create composite films. Subsequently, the viscoelastic features of the film coatings were evaluated.

## 2. Experimental

### 2.1. Materials

Castor oil (CO) supplied from a local market was dehydrated in an oven at 70-80 °C under vacuum for 24 h before use. Isophorone diisocyanate (IPDI), 2-hydroxyethyl methacrylate (HEMA), benzophenone, triethanolamine (TEA), Dimethylolpropionic acid (DMPA), acetone, dibutyltin dilaurate (DBTDL) were purchased from MERC Co., Germany.

### 2.2. Characterization

To analyze the chemical structure of the cross-linker oligomer, FT-IR spectroscopy was used with Perkin Elmer device (USA) in the range of 400-4000  $\text{cm}^{-1}$ . Particle size of the cross-linker dispersed in water was determined by photo scattering (Laser) based on pattern of photo refraction on the detector using Malvern Mastersizer 2000 (England). Dynamic mechanical thermal analyzer (DMTA) was used to study the effect of heat on the viscoelastic properties of the synthesized coatings using DMA device, model 242 C (Netzch Co., Germany). For this, rectangular film coatings were prepared (4×20 mm). Measurements were done in the range of -100 to 120 °C at constant frequency. In the range of  $10^3$  to  $10^6$  MPa, this device is able to analyze the viscoelastic behavior of the polymers.

### 2.3. Preparation of cross-linker oligomer

At first, 6g DMPA, 15 g CO, 0.2 mL DBTDL as a catalyst, and 10 mL acetone were charged into a four-necked balloon containing a thermometer, a magnetic stirrer, a nitrogen inlet, and a condenser. After increasing the temperature to 75 °C in an oil bath, 16.67 g IPDI was dropwise added into the reaction mixture within 30 min. The mixture was then agitated for 3 h at 75 °C. Next, 9.76 g HEMA and 0.2 mL DBTDL were loaded dropwise into the reaction mixture and the blending of the mixture continued for 3 h at 80 °C. In this step, as expected, hydroxyl groups of HEMA completely reacted with isocyanate groups and terminated C=C bonds. At the end, the reaction mixture

was cooled to 40 °C. Finally, 7.46 g TEA was added to the reaction container to neutralize and prepare the water-soluble mixture. The synthesis process of the cross-linker oligomer is shown in Figure 1.

## 2.4. Preparation of PUAW composite coatings

UV-curable urethane acrylate (PUA) resin was prepared and characterized as discussed in the previous literature [23]. First, in order to evaporate the water, the synthesized cross-linker oligomer was set for 12 h in an oven at 65 °C. On the other hand, 5 g PUA resin was separately poured into four beakers. Then, 0, 2, 4 and 6 wt% of the synthesized cross-linker was added to each beaker. Afterwards, at 65 °C, the mixtures were dispersed by a magnetic stirrer at 1100 rpm for 4 h. Then, benzophenone and triethanolamine as photo-initiator and co-initiator (both 0.5wt% of resin), respectively, were added to each mixture in order to prepare the mixtures to participate in the radical polymerization. Each mixture was again dispersed for 20 min. Ultimately, 120  $\mu\text{m}$  thick films were prepared on several glassy molds by a film applicator. The prepared films were exposed to a UV lamp (Hg, 1kW, 80 w/cm) for 120 s [24, 25]. The obtained thin composite film coatings were coded as PUAW 0wt%

(pure sample), PUAW 2wt%, PUAW 4wt%, and PUAW 6wt%.

## 3. Results and Discussion

### 3.1. FT-IR of cross-linker oligomer

Figure 2 represents the main FT-IR spectrum of the synthesized cross-linker. According to Figure 2, there is no absorption band in the 2250-2280  $\text{cm}^{-1}$  range mentioning the fact that -NCO groups have reacted completely with hydroxyl (-OH) groups of DMPA and HEMA. The wide peak at 3379  $\text{cm}^{-1}$  is pertained to the stretching vibrations of -NH. The C-H stretching vibrations in  $\text{CH}_2$  and  $\text{CH}_3$  are seen at 2925 and 2851  $\text{cm}^{-1}$ , respectively. The absorption peak attributed to the C=O ester group stretching vibrations related to urethane and castor oil, is observed at 1725  $\text{cm}^{-1}$ . The perceived absorption peaks at 1532 and 1460  $\text{cm}^{-1}$  are pertained to bending vibrations of N-H and C-H, respectively. The absorption bands at 1302 and 1160  $\text{cm}^{-1}$  indicate C-O and C-N stretching vibrations of urethane. Also, the absorption peak observed at 1028  $\text{cm}^{-1}$  corresponds to the C-O stretching vibrations in HEMA [23, 26, 27]. The findings confirm that the cross-linker oligomer has been synthesized successfully.

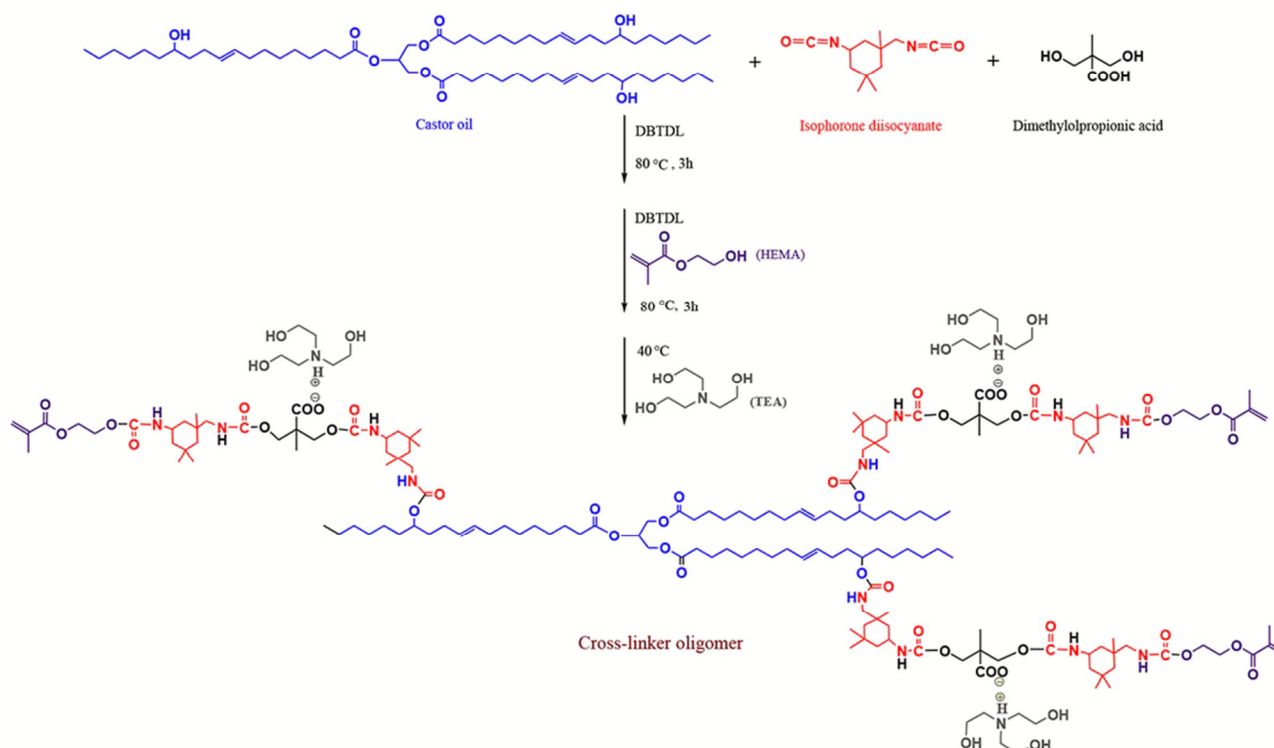


Figure 1: The synthesis process of cross-linker oligomer.

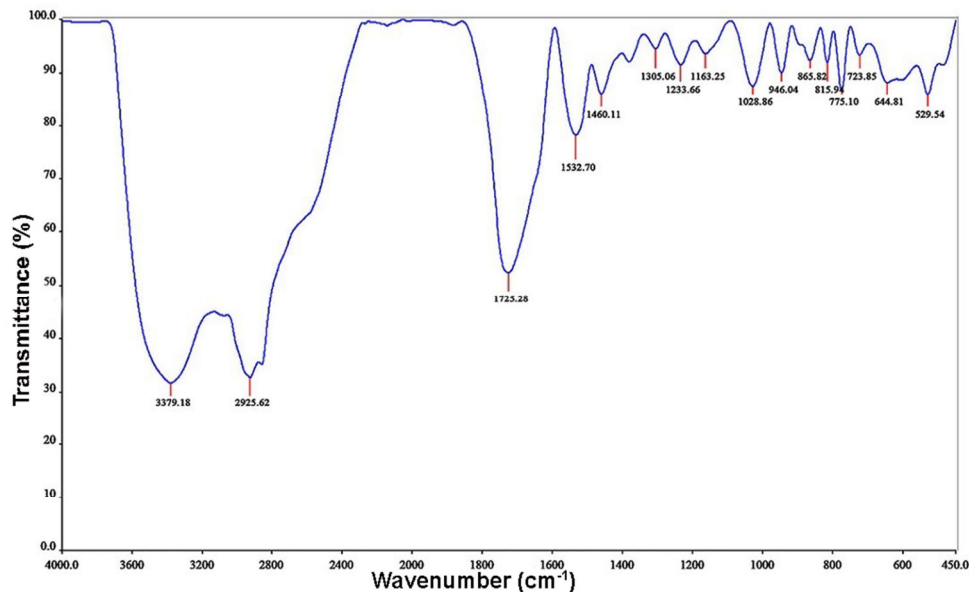


Figure 2: FT-IR spectrum of cross-linker oligomer.

### 3.2. Particle size distribution

The analysis of particle size is considered as an important method to evaluate the persistence of distribution of the particles which is totally recognized by the smaller particles size. Particle size distribution is dependent on the polymerization method, blending speed, kind of cross-linker in terms of hydrophilicity or hydrophobicity, and the solubility of the polymer compounds. The plot of particle size versus volume percent of the mixture is shown in Figure 3. According to Figure 3, the existence of polar groups in the cross-linker caused the dissolution and dispersion of the cross-linker particles in water, so that more particles

with the size of 70.93  $\mu\text{m}$  were homogeneously dispersed in the mixture. Additionally, the decrease in size of the distributed particles in the aqueous phase led to a decrease in cohesion, coagulation, and sedimentation of the particles. Therefore, one could conclude that, the prepared cross-linker is a hydrophile compound in which dispersion of particles increases in the emulsion after dissolving in water. In the surface polymer coatings, although the larger particles dry quickly, the smaller particles are more proper than the larger ones owing to necessity of the deep penetration of dispersion in the matrix [28, 29].

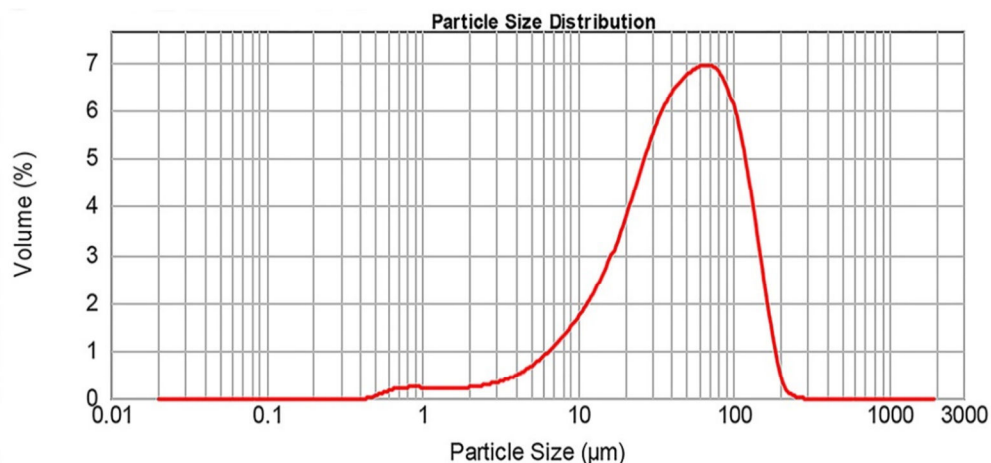


Figure 3: Particle size distribution of the synthesized cross-linker.

### 3.3. Viscoelastic properties

#### 3.3.1. Storage modulus

In the dynamic mechanical examination, storage modulus ( $E'$ ) is an indicative of the substance elasticity, and shows the substance ability to maintain the stored energy. As a temperature function,  $E'$  of PUAW film coatings with 0, 2, 4 and 6 weight percentages was measured. The variation of  $E'$  of the PUAW film coatings with temperature is presented in Figure 4. It can be seen that all  $E'$  values increase up to  $-80\text{ }^{\circ}\text{C}$ . However, by further increasing the temperature,  $E'$  decreases, so that from  $0\text{ }^{\circ}\text{C}$  on, a severe drop in storage modulus takes place. At temperatures higher than  $50\text{ }^{\circ}\text{C}$ ,  $E'$  falls sharply. The  $E'$  decrease in the glass-rubber transition region at about  $50\text{ }^{\circ}\text{C}$  could be discussed based on the movement of the polymer chains in the glass transition temperature ( $T_g$ ) region. Since, polymer is rigid and glassy at temperatures below  $T_g$ , storage modulus decreases beyond the glass-rubber transition region. Adding cross-linker to the matrix of the polymers leads to the increase in  $T_g$ . Because of this reinforcement effect of the cross-linker,  $E'$  of the films decreases less than that of the net polymer. Accordingly, the reinforcement effect of the cross-linkers with a higher cross-link density (4 and 6 wt%) is more tangible in the rubber region. The

increase in  $E'$ , as the amount of the cross-linker increases to 6wt%, is an indicative of the better tension conductivity between the cross-linker and the polymer matrix at higher temperatures, great physical and chemical interactions, and strong connections between the cross-linker and the polymer matrix [30, 31].

#### 3.3.2. Loss modulus

Figure 5 represents the loss modulus ( $E''$ ) graphs of the PUAW films at the temperature range under study. According to Figure 5, with an increase in the temperature, loss modulus increases, and then, it drops. A sharp increase in the loss modulus is an indication of the enhancement of excitability in the polymer structure caused by glass-rubber transition that never occurs at temperatures below  $T_g$ . At  $20\text{--}40\text{ }^{\circ}\text{C}$ , peak height of  $E''$  curves of all the samples rises up to the maximum point, this is because of lessening in excitability of the polymer chains [32]. The loss modulus peak reveals the maximum waste of the mechanical energy. In the PUAW 6wt%, the loss modulus curve is seen on the lowest height at  $25\text{ }^{\circ}\text{C}$  that indicates energy is wasted less than the other samples. The fact behind this is an increase in the thermal resistance through the transverse connections between PUAW 6wt% and the resin matrix.

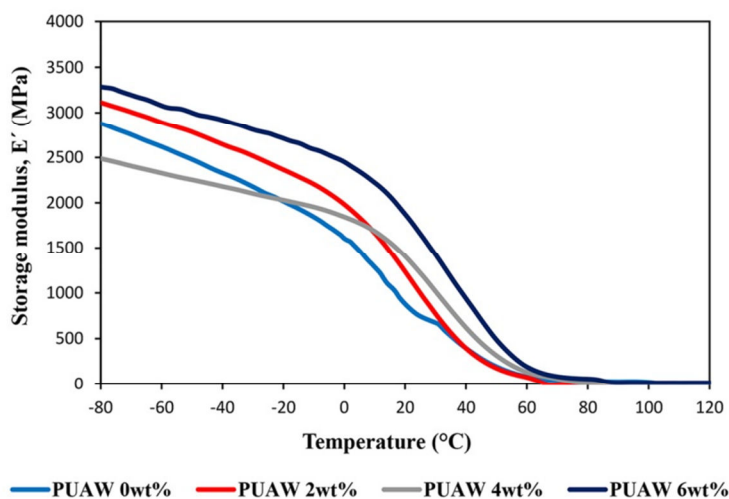


Figure 4:  $E'$  curves for PUAW films.

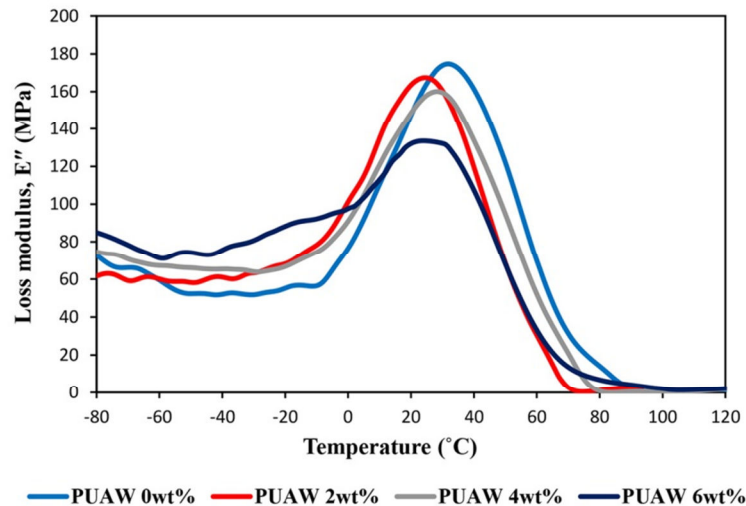


Figure5: E'' curves for PUAW films.

### 3.3.3. Loss tangent

Loss tangent ( $\tan \delta$ ) curves for PUAW film coatings are indicated in Figure 6. The  $\tan \delta$  peak for all the samples is obtained at temperatures higher than 50 °C, as shown in Figure 6.  $\tan \delta$  curve of the PUAW 6wt% film shifts to higher temperature compared to the PUAW 2wt% and PUAW 4wt% films. Its height is also less than that of the two other samples. One main use of DMTA is to measure  $T_g$  for polymers. The highest point in the  $\tan \delta$  curve implies  $T_g$ . At temperatures higher than  $T_g$ , polymers show elastic features, the viscosity increases, and the stiffness drops considerably. In the  $T_g$  region,  $E'$  decreases sharply and loss modulus reaches its maximum value. An organic or inorganic filler or reinforcer could change  $T_g$ . The lower  $T_g$  pertains to flexible polymers and the higher  $T_g$  pertains to rigid polymers [33]. As can be seen, the PUAW 6wt% film shows more flexibility than the sample with no cross-linker (PUAW 0wt%), and more stiffness compared to other samples. The reasons are discussed in the following paragraphs. In the polymer composites, loss tangent is influenced by the reinforcement phase, so as by adding the reinforcer, loss tangent of the composites is reduced relative to the pure polymer. This can be attributed to the limitation of the polymer molecules movement in the presence of 4 and 6 wt% cross-linkers. The other cause is reduction in matrix in the composites containing reinforcer. As the reinforcer increases, the matrix ratio decreases in the prepared composite. By declining the matrix, the

number of moving units drops which create the relaxation process, and in the following, the moving units disconnect, then, the surface under the curve becomes smaller. With an increase in the cross-linker in the prepared composite formulation,  $\tan \delta$  is lessened, and the height of the curve peak decreases. Since in the dynamic-mechanical examination, the loss of mechanical energy takes place on the common surface of cross-linker and matrix, one could expect the strong interactions on this surface reduce the wasted energy, accordingly, the lowering of height of the peak of  $\tan \delta$  is a sign of the better quality of the common surface [34-36]. As a result, adding the synthesized cross-linker, to the resin matrix (especially for PUAW 6wt%) results in the improvement of viscoelastic characteristics of the composites.

### 3.3.4. Cross-link density

The DMTA data such as  $E'$  in the rubber region and curve peak of  $\tan \delta$  could be straightly used to measure the cross-link density. Cross-link density ( $\nu_e$ ) of PUAW coatings is calculable by Equation (1) [37, 38]:

$$\nu_e = \frac{E'}{3RT} \quad (1)$$

Where  $E'$  is storage modulus,  $R$  is the universal gas constant, and  $T$  is the absolute temperature in K. Findings of equation 1 are summarized in Table 1 and Figure 7. It can be concluded that by adding the cross-linkers to the PUA resin matrix, cross-link density of the

PUAW composites increases due to, the increase in  $E'$  in the rubber region and the reduction in peak height of the  $\tan \delta$  curve, so that by a rise in concentration of the cross-linker in the resin matrix, the cross-link density is also increased. The maximum value of the computed cross-link density belongs to PUAW 6wt%. When the mixture of resin and cross-linker containing double

bonds is exposed to the UV irradiation, a great deal of the polymer participates in the radical hydrogen abstraction polymerization. Then, strong chemical bonds are formed in three dimensions causing cross-link density to be increased for the coatings containing more cross-linker [21, 31, 39].

**Table 1:** Changes of cross-link density in PUAW composites.

| Samples   | $T_g$ (°C) | $E'$ (MPa) | Crosslink density (mol/m <sup>3</sup> ) |
|-----------|------------|------------|---|
| PUAW 0wt% | 65.6       | 110        | 11534                                   |
| PUAW 2wt% | 55.7       | 107        | 13102                                   |
| PUAW 4wt% | 58.1       | 159        | 19362                                   |
| PUAW 6wt% | 60.5       | 174        | 20954                                   |

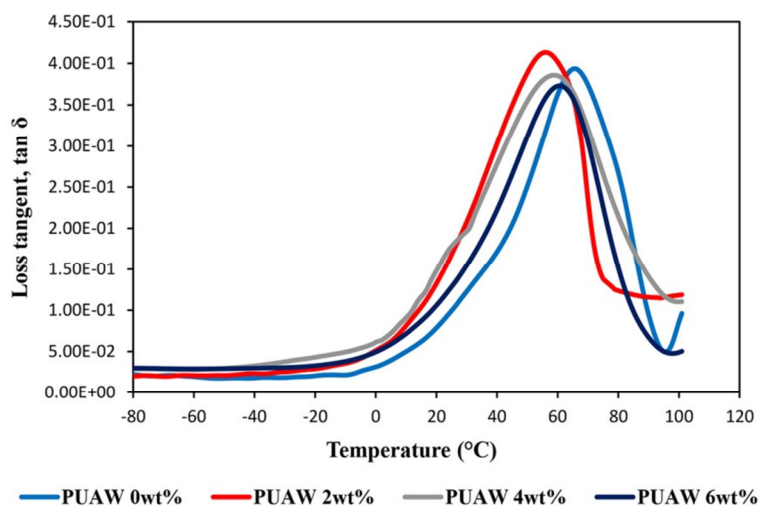


**Figure 6:** Tan  $\delta$  curves for PUAW films.

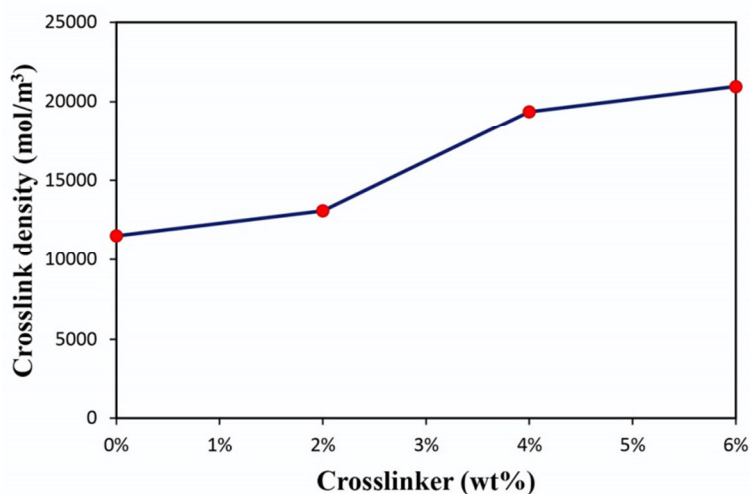


**Figure 7:** Changes of cross-link density in terms of cross-linker wt%.

#### 4. Conclusion

In the present study, bio-based composite coatings were prepared using PUA resin and different amounts of UV-curable tri-functional castor oil-based waterborne urethane acrylate as a bio-friendly cross-linker. To examine the reaction progress between hydroxyl and isocyanate groups and to analyze the chemical structure of the synthesized cross-linker oligomer, FT-IR test was used. By the particle size analysis, persistence of distribution of the cross-linker particles was estimated. As the results showed, cross-linker particles were homogeneously distributed in the emulsion with appropriate stability. Subsequently, viscoelastic properties of the composites were analyzed using DMTA test. The findings signified that adding

different weight percentages of the cross-linkers to the PUA resin resulted in the formation of films with proper thermal-mechanical features. Samples containing cross-linker had higher storage modulus, stability and excellent elastic feature at high temperatures. With the cross-linker increase in the composite coatings,  $T_g$  was raised, too, therefore, the maximum value of  $T_g$  belonged to PUAW 6wt%. However,  $T_g$  of the sample without cross-linker was higher than that of the samples with cross-linker, confirming the flexibility of the coatings containing cross-linker. DMTA data showed that, adding cross-linker to the resin matrix increased the cross-link density of the films. As a result, PUAW 6w% possessed the maximum cross link density.

#### 5. References

1. X. G. Dang, C. H. Yuan, H. Z. Shan, An eco-friendly material based on graft copolymer of gelatin extracted from leather solid waste for potential application in chemical sand-fixation, *J. Clean. Prod.*, 188(2018), 416-424.
2. M. A. R. Meier, J. O. Metzgerb, U. S. Schubert, Plant oil renewable resources as green alternatives in polymer science, *Chem. Soc. Rev.*, 36(2007), 1788-1802.
3. S. Chen, C. Ma, G. Zhang, Biodegradable polymer as controlled release system of organic antifoulant to prevent marine biofouling, *Prog. Org. Coat.*, 104(2017), 58-63.
4. S. Oprea, P. Gradinariu, V. Oprea, Properties and fungal biodegradation of the different cellulose derivatives structure included into castor oil-based polyurethane composites, *J. Compos. Mater.*, 53(2019), 3535-3548.
5. S. S. Panda, S. K. Samal, S. Mohanty, and et al, Preparation, characterization, and properties of castor oil-based flexible polyurethane/Cloisite 30B nanocomposites foam, *J. Compos. Mater.*, 52(2018), 531-542.
6. A. Madhi, B. Shirkavand Hadavand, A. Amoozadeh, Synthesis, characterization and study on thermal stability, mechanical properties and thermal conductivity of UV-curable urethane acrylate Clay (MMT) nanocomposites, *J. Appl. Chem.*, 12(2018), 91-98.
7. Z. Hesari, B. Shirkavand Hadavand, M. Mahmoodi Hashemi, Fabrication and study of structural, optical and electrical properties of UV curable conductive polyurethane acrylate films containing polyaniline- $\text{Co}_3\text{O}_4$  nanocomposites, *Prog. Color Colorants Coat.*, 9(2016), 41-52.
8. A. Madhi, B. Shirkavand Hadavand, A. Amoozadeh, Thermal conductivity and viscoelastic properties of UV-curable urethane acrylate reinforced with modified  $\text{Al}_2\text{O}_3$  nanoparticles, *Prog. Color Colorants Coat.*, 10(2017), 193-204.
9. S. Kasetaitė, J. Jolita Ostrauskaitė, V. Grazulevičienė, and et al, Biodegradable glycerol-based polymeric composites filled with industrial waste materials, *J. Compos. Mater.*, 51(2017), 4029-4039.
10. A. Corma, I. Sara, V. Alexandra, Chemical routes for the transformation of biomass into chemicals, *Chem. Rev.*, 107(2007), 2411-2502.
11. T. Gurunathan, R. Arukula, High performance polyurethane dispersion synthesized from plant oil renewable resources: a challenge in the green materials, *Polym. Degrad. Stab.* 150(2018), 122-132.
12. M. A. Mosiewicki, G. A. Dell'Arciprete, M.I. Aranguren, and et al, Polyurethane foams obtained from castor oil-based polyol and filled with wood flour, *J. Compos. Mater.*, 43(2009), 3057-3072.
13. T. Gurunathan, S. Mohanty, S. K. Nayak, Isocyanate terminated castor oil-based polyurethane prepolymer: Synthesis and characterization, *Prog. Org. Coat.*, 80(2015), 39-48.
14. S. S. Panda, B. P. Panda, S. Mohanty S, and et al, Synthesis and properties of castor oil-based waterborne polyurethane Cloisite 30B nanocomposite coatings, *J. Coat. Technol. Res.*, 14(2017), 377-394.
15. M. A. Alaa, K. Yusoh, S. F. Hasany, Synthesis and characterization of polyurethane-organoclay nanocomposites based on renewable castor oil polyols, *Polym. Bull.* 72(2015), 1-17.
16. F. Mohtadizadeh, M. J. Zohuriaan-Mehr, B. Shirkavand Hadavand, and et al, Tetra-functional epoxy-acrylate as crosslinker for UV curable resins: Synthesis, spectral, and thermo-mechanical studies, *Prog. Org. Coat.*, 89(2015), 231-239.



17. S. D. Reinitz, E. M. Carlson, R. A. C. Levine, and et al, Dynamical mechanical analysis as an assay of cross-link density of orthopaedic ultrahigh molecular weight polyethylene, *Polym. Test.*, 45(2015), 174-178.
18. W. Stark, M. Jaunich, Investigation of ethylene/vinyl acetate copolymer (EVA) by thermal analysis DSC and DMA, *Polym. Test.*, 30(2011), 236-242.
19. W. Stark, Investigation of the curing behaviour of carbon fibre epoxy prepreg by Dynamic Mechanical Analysis DMA, *Polym. Test.*, 32(2013), 231-239.
20. H. Farzad, F. Najafi, M. Bengisu, and et al, Synthesis and characterization of aliphatic tri-functional oligomeric urethane methacrylate used for UV-curable aluminum pigmented coatings., *J. Macromol. Sci. Part A.*, 50(2013), 504-512.
21. J. Mohammadian, B. Shirkavand Hadavand, S. Khajenoori, Synthesis and Investigation on Viscoelastic Properties of Urethane Acrylate-Polyaniline, *Prog. Color Colorants Coat.*, 11(2018), 241-252.
22. B. Shirkavand Hadavand, F. Najafi, M. R. Saeb, and et al, Hyperbranched polyesters urethane acrylate resin: A study on synthesis parameters and viscoelastic properties., *High. Perform. Polym.*, 29(2017), 651-662.
23. A. Madhi, B. Shirkavand Hadavand, Eco-friendly castor oil-based UV-curable urethane acrylate zinc oxide nanocomposites: Synthesis and viscoelastic behavior, *J. Compos. Mater.* 54(2019), 101-110.
24. F. Najafi, E. Bakhshandeh, B. Shirkavand Hadavand, and et al, Toward UV-curable urethane acrylate/silica hybrid coatings: Introducing urethane methacrylate trimethoxysilane (UAMS) as organic-inorganic coupling agent, *Prog. Org. Coat.*, 77(2014), 1957-1965.
25. A. Majeed, E. Yousif, G. A. El-Hiti, D. S. Ahmed, A. A. Ahmed, Stabilization of Poly (vinyl chloride) containing captopril tin complexes against degradation upon exposure to ultraviolet light, *J. Vinyl. Addit. Technol.*, 2020. DOI: 10.1002/vnl.21774.
26. V. Mishra, I. Mohanty, M.R. Patel, and et al, Development of Green Waterborne UV-Curable Castor Oil-Based Urethane Acrylate Coatings: Preparation and Property Analysis, *Int. J. Polym. Anal. Char.*, 20(2015), 504-513.
27. H. Liu, M. Dong, W. Huang, and et al, Lightweight conductive graphene/thermoplastic polyurethane foams with ultrahigh compressibility for piezoresistive sensing, *J. Mater. Chem. C.*, 5(2017), 73-83.
28. F. Najafi, B. Akbari, F. Najafi, and et al, Characterization of the physical-mechanical properties of dental resin composites reinforced with novel micro-nano hybrid silica particles: An optimization study, *Macromol. Sci. Part A.*, 55(2018), 736-746.
29. B. Ghobadi Jola, B. Shirkavand Hadavand, K. Didehban, A. Mirshokraie, The Effect of Molecular Weight of Polyethylene Glycol and Nanoclay Percentages on the Rheological Behavior of Dispersing Anionic Polyurethane Nanocomposites, *J. Inorg. Organomet. Polym.*, 28(2018), 92-101.
30. A. Madhi, B. Shirkavand Hadavand, A. Amoozadeh, UV-curable urethane acrylate zirconium oxide nanocomposites. Synthesis, study on viscoelastic properties and thermal behavior, *J. Compos. Mater.*, 52(2018), 2973-2982.
31. B. Shirkavand Hadavand, M. Pishvaei, M. Hosseiniiasari, The role of nanoclay on surface roughness and characteristics of epoxy polysulfide nanocomposite, *Prog. Org. Coat.*, 131(2019), 60-66.
32. S. K. Samal, S. Mohanty, S. K. Nayak, Polypropylene bamboo/glass fiber hybrid composites: Fabrication and analysis of mechanical, morphological, thermal, and dynamic mechanical behavior, *J. Reinf. Plast. Compos.*, 28(2009), 2729-2748.
33. B. Shirkavand Hadavand, H. Hosseini, Investigation of viscoelastic properties and thermal behavior of photocurable epoxy acrylate nanocomposites, *J. Sci. Eng. Compos. Mater.* 24(2017), 691-697.
34. L. U. Devi, S. S. Bhagawan, S. Thomas, Dynamic mechanical analysis of pineapple leaf/glass hybrid fiber reinforced polyester composites, *Polym. Compos.*, 31(2010), 956-965.
35. H. L. Ornaghi, S. H. P. da Silva, A. J. Zattera, Hybridization effect on the mechanical and dynamic mechanical properties of curaua composites, *Mater. Sci. Eng A.*, 528(2011), 7285-7289.
36. A. Hassan, N. A. Rahman, R. Yahya, Extrusion and injection-molding of glass fiber/ MAPP/polypropylene: Effect of coupling agent on DSC, DMA and mechanical properties, *J. Reinf. Plast. Compos.*, 30(2011), 1223-1232.
37. L. Song , Q. Ye, X. Ge, and et al, Synthesis and evaluation of novel dental monomer with branched carboxyl acid group, *J. Biomed. Mater. Res. Part B.*, 102(2014), 1473-1484.
38. V. V. Krongauz, Diffusion in polymers on crosslink density Eringappoarch mechanism, *J. Them. Ana. Calorim.*, 102(2010), 435-445.
39. A. Madhi, B. Shirkavand Hadavand, Bio-based UV-curable urethane acrylate graphene nanocomposites: synthesis and properties, *SN Appl Sci.*, 2020. DOI: 10.1007/s42452-020-2527-4.

How to cite this article:

A. Madhi, B. Shirkavand Hadavand, Tri-functional Bio-friendly Cross-linker for UV-Curable Coatings: Synthesis and Study of Viscoelastic Properties. *Prog. Color Colorants Coat.*, 14 (2021), 199-207.

